

Polysaccharide from Loquat Leaves to Prepare Hierarchical Porous Carbon as a Matrix for Active Sulfur

Luo Rui, Xiong Shenglin*

Key Laboratory of the Colloid and Interface Chemistry, Ministry of Education, School of Chemistry and Chemical Engineering, Shandong University, Jinan 250100, P. R. China

(Received 15 June 2018; revised 25 June 2018; accepted 9 July 2018)

Abstract: Fossil fuel exhaustion and overdevelopment usually lead to a recession, which is worsened by the environmental pollution. So it is of high priority to develop high-efficiency energy storage device. Here, a green and environment-friendly strategy is devised to fabricate carbon materials from biomass. By water extraction and alcohol precipitation, polysaccharide is extracted from loquat leaves. After calcining under high temperature, hierarchical porous carbon materials (HPCM) are obtained, possessing a variety of macropores, mesopores and micropores. Such ample and hierarchical pores enable the electrolyte infiltration and the buffering of the volume expansion of sulfur in repeated electrochemical reactions. The structure stability of the entire electrode can thus be well maintained. When evaluated as the scaffold for sulfur, the electrochemical performance of carbon/sulfur composite was tested. Even after 500 cycles, the reversible capacity is retained as high as 485.4 mA · h/g at the current density of 1.6 A/g. It also offers a notable rate capability, attaining the discharge capacity of 700.7 mA · h/g at 2 C. All the electrochemical performance results prove the feasibility of the proposed strategy.

Key words: energy storage; loquat leaves; hierarchical porous carbon materials

CLC number: O611.4 **Document code:** A **Article ID:** 1005-1120(2018)04-0611-08

0 Introduction

Our environment is facing energy crisis, referred to the economic impact caused by the shortage of energy supply or the rise of prices. This usually involves shortages of oil, electricity or other natural resources. Human beings are actively and extensively exploiting the energy resources to be popularized, such as solar energy, geothermal energy, wind energy, marine energy, biomass energy and nuclear fusion energy. However, those natural energy sources are variable, intermittent, and heavily depend on the location, season. It is of high urgency to develop renewable energy resources for sustainability. The secondary batteries are coming into scientists' view. Among them, lithium-sulfur batteries (LSBs) are regarded as one of the most promising secondary battery systems because of their high theoretical

specific capacity and energy density^[1-6]. With the continuous progresses of science and technology, more Li-S anode materials have been developed. However, LSBs currently face many challenges, including volume variation and the intrinsically poor electronic conductivity of sulfur^[2,6]. Hence, great efforts have been needed to explore the effective strategies to solve issues.

To the best of our knowledge, carbon materials are widely used in many fields, including supercapacitors, lithium-air batteries, and catalysis, because of their large specific surface area, excellent conductivity and good chemical stability^[7-8]. The electrochemical performance of LSBs can be improved effectively by constructing suitable carbon materials with hierarchical pore structure and composite cathode material. Lucid waters and lush mountains are invaluable assets. It

*Corresponding author, E-mail address: chexls@sdu.edu.cn.

is of positive significance to replace traditional chemical reagents with low cost and environment-friendly biomass raw materials^[9-11]. Wu et al. reported four kinds of biomass carbon materials derived from mushroom by a facile activation method using H_3PO_4 , K_2CO_3 , KOH and ZnCl_2 as activators. Moreover, the correlations between micro-morphology characteristics and electrochemical properties have been systematically investigated^[12]. Yu group prepared the hair-derived carbon/sulfur composite via a ready melt-diffusion method, followed by wrapping with reduced graphene oxide (rGO) sheets by electrostatic self-assembly^[13]. Highly porous activated carbon foam (ACF) with micromesoporosity has been synthesized through the carbonization of pomelo peel and activation by KOH ^[14], which showed the remarkable performance as the cathode supporter for rechargeable lithium-sulfur batteries. Hence, the derivation of carbon materials from different biomass can enable the microstructure and composition of the resulting carbon. Furthermore, from the viewpoint of environmental protection and efficiency, we are committed to developing an environmentally friendly and efficient sulfur matrix.

Herein, we adopted the method of water extraction and alcohol precipitation to extract polysaccharide from loquat leaves. Followed by the calcination under the condition of high temperature, hierarchical porous carbon materials (HPCM) were attained with a feature of the co-existence of macropores, mesopores and micropores. Abundant and hierarchical pores are favorable for offering space of volume expansion in the repeated process of charging and discharging, benefiting the structure stability of the entire electrode. When evaluated as the scaffold for sulfur, the electrochemical performance of carbon/sulfur composite was tested. Even after 500 cycles, the reversible capacity is retained as high as $485.4 \text{ mA} \cdot \text{h/g}$ at the current density of 1.6 A/g . It also offers a notable rate capability, attaining the discharge capacity of $700.7 \text{ mA} \cdot \text{h/g}$ at 2 C . All the electrochemical performance results

prove the feasibility of our strategy.

1 Experiment

1.1 Sample preparation

Experimental chemicals include loquat leaves, sublimed sulphur (G. R, Aladdin) and anhydrous ethanol (A. R, Sinopharm chemical reagent Co., Ltd).

Polysaccharide can be extracted from loquat leaves as follows^[15]. First, the clean loquat leaf will be shredded. Then, 4 g crushed loquat leaves were put into a glass beaker, followed by pouring 100 ml of ultrapure water and stirring in the water bath at $90 \text{ }^\circ\text{C}$ for 2 h. After that, it was cooled to room temperature. Through the filtration, the filtrate was collected. Then, the filter residue was extracted for the second time. Then, the filtrate obtained twice was mixed together. The supernatant was concentrated via centrifugation and evaporated to about 50 mL, followed by adding four-fold anhydrous ethanol. Then it was standing still at $4 \text{ }^\circ\text{C}$ for 12 h, filtered and washed for several times. The powder was dried to get polysaccharide.

The extracted polysaccharide was heated at $400 \text{ }^\circ\text{C}$ for 2 h in Ar atmosphere with a heating rate of $2 \text{ }^\circ\text{C}/\text{min}$ and then at $900 \text{ }^\circ\text{C}$ for 3 h with a heating ramping of $4 \text{ }^\circ\text{C}/\text{min}$. The final sample was washed with 1 mol/L hydrochloric acid to rid the impurities and dried at $60 \text{ }^\circ\text{C}$.

The obtained HPCM and sublimed sulfur were accurately weighed based on a certain mass ratio and mixed fully. Then, it was put into a sealed container and heated at $155 \text{ }^\circ\text{C}$ for 12 h to obtain HPCM/S composite.

1.2 Sample characterization

The morphology and microstructure of the samples were characterized by various devices. X-ray powder diffraction (XRD) patterns were collected on an X-ray diffractometer (Bruker D8, $2\theta=10^\circ-80^\circ$). The structural images were recorded on field emission scanning electron microscopy (FESEM, JSM-7600F) and transmission electron microscopy (TEM, JEM-1011). The N_2 ad-

sorption isotherms were tested by micromeritics ASAP-2020HD88 at degassing temperature of 200 °C. The loading content of sulfur was tested by a Mettler Toledo TGA/SDTA851 thermal analyzer with a heating rate of 10 °C/min in N₂ atmosphere. Raman spectra were obtained using the NEMUS670 spectrometer.

1.3 Electrochemical measurements

First, HPCM/S, acetylene black, carbon nanotubes and PVDF were mixed based on a mass ratio of 70 : 12 : 10 : 8. Then N-Methyl pyrrolidone (NMP) was added dropwise and stirred for a short time to make a slurry. The homogeneous slurry obtained was coated on the aluminum foil and dried at 60 °C for 10 h, followed by cutting into disks with a diameter of 12 mm. On each disk, the areal loading of sulfur is about 1.0 mg/cm². The CR2016 coin-type cells were assembled in the glovebox filled with Ar gas. The electrolyte was a 1 M bis(trifluoromethane) sulfonamide lithium salt dissolved in 1,3-dioxolane/1,2-dimethoxyethane (DOL/DME, volume ratio = 1 : 1) with 2% (in weight) LiNO₃ as additive. The lithium foil was used as counter electrode in addition with modified or unmodified Celgard 2400 membrane as the separator. The cyclic voltammetry (CV) profiles were detected using an electrochemical workstation (CHI 760E) at a scan rate of 0.1 mV/s. The charge-discharge performances of Li-S cells were collected by a LAND CT2001A testing system within a voltage window between 1.7 V and 2.8 V.

2 Results and Discussion

2.1 Morphology and structure of samples

Fig. 1 presents TEM and FESEM images of HPCM. As we can see, the HPCM is a typically porous carbon network composed of particles stacking together. The porous structure formed by the interconnection between particles can be clearly seen in Figs. 1(b–d). Such porous structures are favorable for the loading and confinement of sulfur. After combination with sublimed sulfur, the composite of HPCM/S is monitored

by electron microscopy. As shown in Fig. 2, compared with the bare HPCM sample, the morphology of HPCM/S hardly varies, demonstrating that the active material is uniformly distributed within the hierarchical pores.

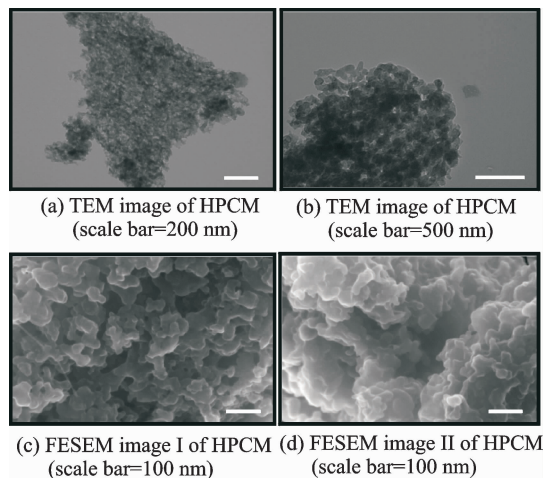


Fig. 1 TEM and FESEM images of HPCM

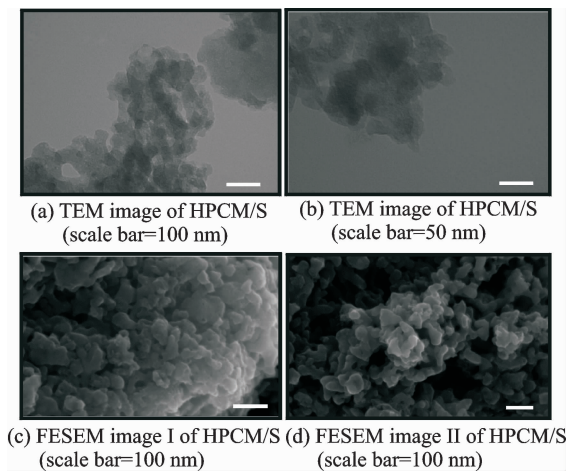


Fig. 2 TEM and FESEM images of HPCM/S

Fig. 3(a) exhibits the XRD pattern of HPCM, HPCM/S and elemental sulfur. It can be clearly seen that HPCM has a wide peak in the range of 20°–30°, characteristic of the amorphous carbon^[16,17]. After sulfur loading, the characteristic peaks of sulfur in HPCM/S composite are weaker than those of pure sulfur. This indicates that most of the elemental sulfur has infiltrated into the pores of the carbon material^[18,19]. However, it is evitable that partial sulfur crystals are attached on the HPCM surface. The exact content of sulfur in HPCM/S composite

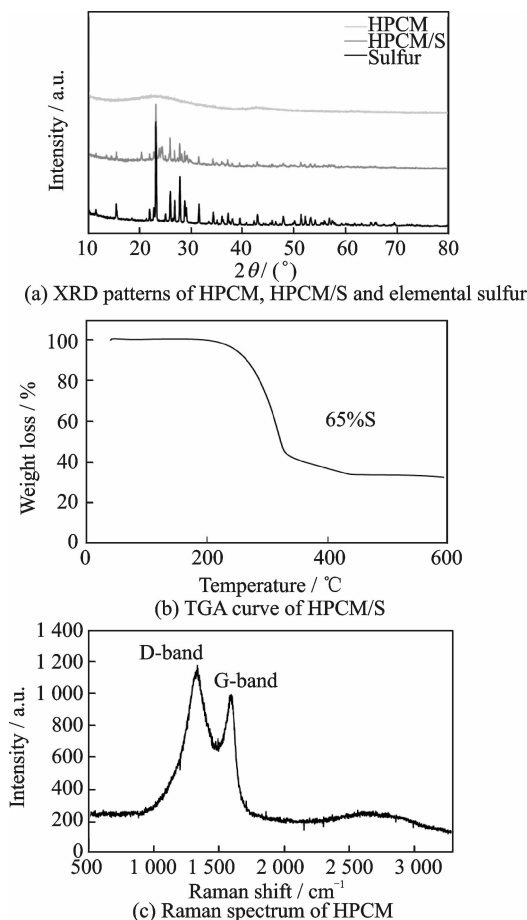


Fig. 3 Structure and phase characterization of HPCM and HPCM/S

was tested by TGA. As displayed in Fig. 3(b), the total mass content of sulfur in the composite is about 65% (in weight). The loss of sulfur in the curve can be notably divided into two stages. A fast tend of weight loss appears from 200 $^{\circ}\text{C}$ to 320 $^{\circ}\text{C}$, which can be attributed to the escaping of sulfur concentrating on the surface or in the pores with relatively big sizes. The second slow stage occurs at higher temperature from 320 $^{\circ}\text{C}$ to 450 $^{\circ}\text{C}$, implying that more energy is required for the sulfur volatilization. This phenomenon accounts for partial sulfur existing in the smaller micropores^[20]. The Raman^[20] spectrum of HPCM is used to detect the graphitization structure of carbon in Fig. 3(c). The D band results from the disordered carbon caused by sp^3 -structured defects, while the G band is typical of sp^2 -hybridized carbon, i. e. graphitic carbon. Three typical peaks are observed to be centered at 1 330, 1 580 and 2 700 cm^{-1} , corresponding to the D, G and

2D bands, respectively. The G peak and the 2D peak indicate that the HPCM has a partially graphitized structure^[21-24].

The adsorption-desorption isotherms over HPCM are displayed in Fig. 4. An intense adsorption happens at the low relative pressure range, which originates from the presence of micropores. Moreover, the H3 type hysteresis is clearly observable, associated with the capillary condensation by mesoporous structures. The corresponding pore size distribution plot (inset of Figs. 4 (a)—(b)) is given based on the Barrett-Joyner-Halenda method. The pores are mainly in the range of 0.75—1.75 nm (micropores), 3.5—5 nm (mesopores) and exceeding 50 nm (macropores), confirming the hierarchical porous structure. After calculation, the BET surface area and total pore volume are 499 m^2/g and 0.63 cm^3/g . Such large specific surface area and pore volume are helpful for the even dispersion of sulfur and anchoring the polysulfides, relieving the volume change of active material during the process of charging or discharging.

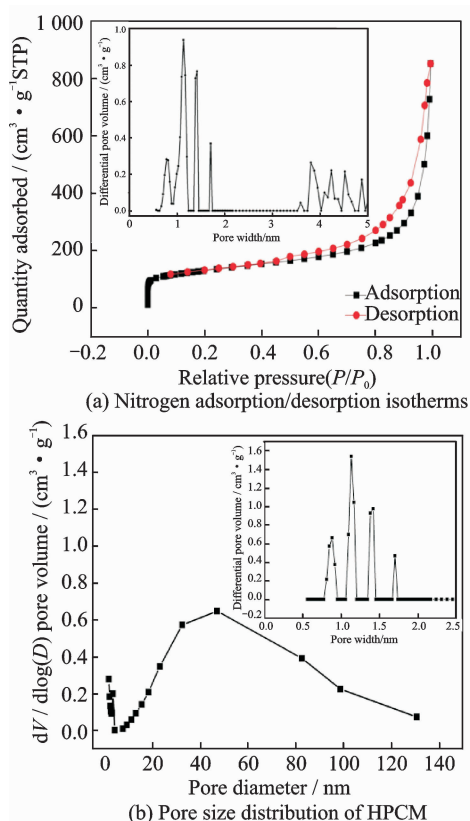


Fig. 4 Porous profile of HPCM

2.2 Electrochemical measurements of HPCM/S

The CR2016 coin-type cells are assembled for testing with the areal loading of sulfur of about 1.0 mg/cm^2 . Fig. 5(a) displays the cyclic voltammogram (CV) charts of HPCM/S in a voltage window of 1.7–2.8 V with a sweep rate of 0.1 mV/s. In the first cathodic scan process, two major broad peaks dominate, which are associated with the two-step sulfur reduction of cyclo- S_8 to Li_2S ^[25–26]. One cathodic peak is at about 2.25 V, corresponding to the sulfur reduction to higher-order polysulfide Li_2S_n ($4 \leq n \leq 8$). The other cathodic peak at about 2 V is related to the further reduction of higher-order polysulfides to Li_2S_2 or Li_2S . In the anodic process, the peak is present at about 2.45 V, which is considered to be attributed to the oxidation reaction of Li_2S to sulfur^[25–27]. From the second loop onwards, the CV curves almost overlap, indicating that the HPCM/S material exhibits good cycling reversibility^[28–29]. The rate performance of the HPCM/S is given in Fig. 5(b). The discharge capacities are 1 012.9, 872.0, 776.2, 700.7 mA · h/g at the current densities of 0.3, 0.8, 1.6 and 3.2 A/g, respectively. When the current density returns to 0.3 A/g, the capacity can recover to 923.0 mA · h/g. The electrode material shows descent rate performance.

Fig. 5(c) describes the galvanostatic charge-discharge profile of HPCM/S hybrid at different rates. It can be found that, as the current rate increases, the voltage gap between discharge and charge plateaus becomes larger, resulting from the more serious polarization^[30–31].

As shown in Fig. 6(a), an initial capacity of 1 146 mAh/g in the first cycle is obtained at a current density of 0.8 A/g. After 300 cycles, stable reversible capacity of 603.5 mAh/g can be maintained, showing the excellent cycling stability. Fig. 6(b) indicates the cycling behavior of HPCM/S at a current density to 1.6 A/g. After the initial activation at 0.5 A/g for 10 cycles, a reversible capacity of 805.7 mA · h/g can be ob-

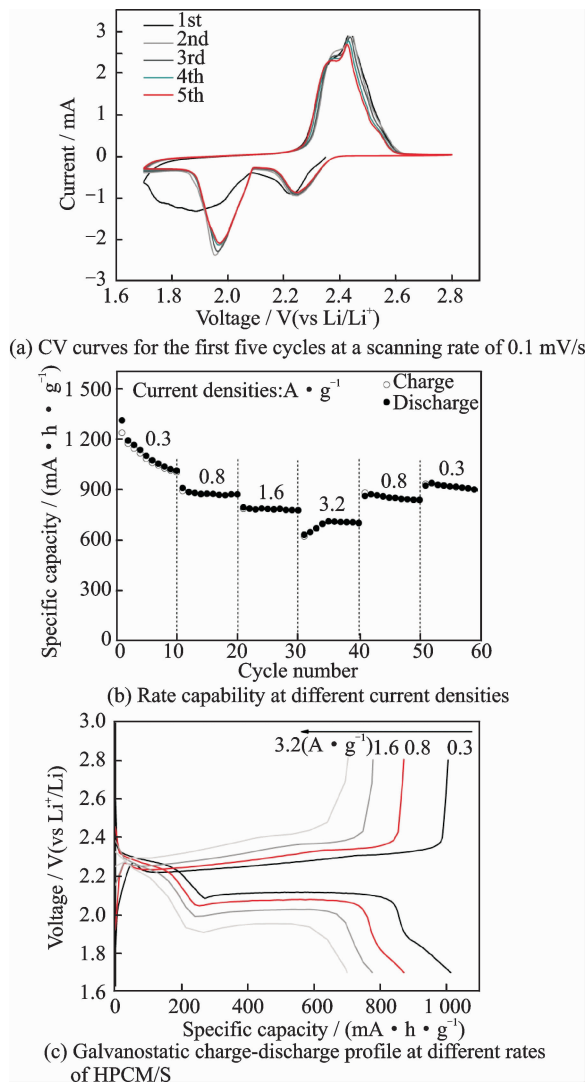


Fig. 5 Electrochemical performance of HPCM/S

tained when the current rate immediately increases to 1.6 A/g. After 500 cycles, the reversible capacity is retained as high as 485.4 mA · h/g. Fig. 6(c) displays the charge-discharge voltage curves of HPCM/S at a current density of 0.8 A/g. After the initial several cycles, the voltage profiles almost have no significant change, which is a token of the excellent reversibility of the electrochemical reactions.

The above analytical results verify that the HPCM/S offers superior rate capability and cycling stability, which is attributed to its advantageous structural features. HPCM possesses higher surface area and pore volume, advantageously rendering the uniform dispersion of active sulfur within the matrix. On the other hand, the elec-

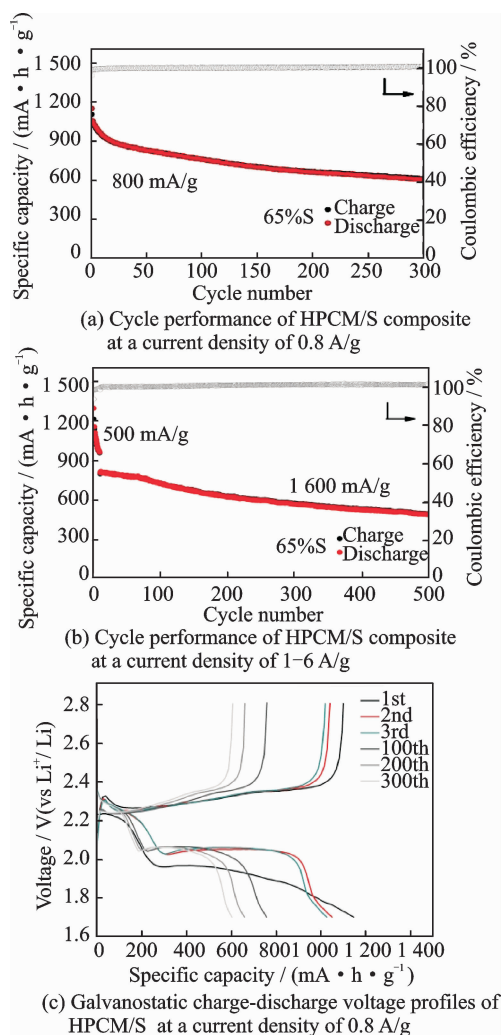


Fig. 6 Cycling behaviors of HPCM/S

trolyte can readily infiltrate and lithium ions can be transported with smaller resistance. In addition, the synergistic effect of macropores, mesopores and micropores can not only effectively fix the active substance sulfur, but also buffer the volume change during charge/discharge process. As a result, higher surface area and hierarchical pores contribute to the improvement of Li-S battery performance.

3 Conclusions

From the perspective of green chemistry, polysaccharide has been extracted from loquat leaves by water extraction and alcohol precipitation. By the following high temperature calcining, the hierarchical porous carbon material was prepared, which includes macropores, mesopores

and micropores. From the electrochemical results, the larger specific surface area, the suitable pore distribution and hierarchical pores make HPCM/S serve as an excellent supporter of sulfur for Li-S batteries. Abundant pores can offer space of volume expansion in the process of charging and discharging, benefiting the structure stability of the entire electrode. Even after 500 cycles, the reversible capacity as high as 485.4 mA · h/g was retained at the current density of 1.6 A/g. This study has explored the feasibility of biomass raw materials for the preparation of sulfur holder, exhibiting the prospective potential for application in Li-S batteries.

Acknowledgements

This work was supported by the Fundamental Research Funds of Shandong University (No. 2016JC033) and the Taishan Scholar Project of Shandong Province (No. ts201511004).

References:

- [1] SEH Z W, SUN Y, ZHANG Q, et al. Designing high-energy lithium-sulfur batteries [J]. *Chemical Society Reviews*, 2016, 45(20):5605-5634.
- [2] ROSENMAN A, MARKEVICH E, SALITRA G, et al. Review on li-sulfur battery systems: An integral perspective [J]. *Advanced Energy Materials*, 2015, 5(16):1500212.
- [3] YIN Y X, XIN S, GUO Y G, et al. Lithium-sulfur batteries: Electrochemistry, materials, and prospects [J]. *Angewandte Chemie International Edition*, 2013, 52(50):13186-13200.
- [4] XU G, DING B, PAN J, et al. High performance lithium-sulfur batteries: Advances and challenges [J]. *Journal of Materials Chemistry A*, 2014, 2(32):12662-12676.
- [5] MANTHIRAM A, FU Y, SU Y S. Challenges and prospects of lithium-sulfur batteries [J]. *Acc Chem Res*, 2013, 46(5):1125-1134.
- [6] YANG Y, ZHENG G Y, CUI Y. ChemInform abstract: Nanostructured sulfur cathodes [J]. *Cheminform*, 2013, 44(24):3018-3032.
- [7] LEE J, KIM J, HYEON T. Recent progress in the synthesis of porous carbon materials [J]. *Advanced Materials*, 2011, 18(16):2073-2094.

- [8] PANDOLFO A G, HOLLENKAMP A F. Carbon properties and their role in supercapacitors [J]. *Journal of Power Sources*, 2006, 157(1):11-27.
- [9] DUTT S, BHAUMIK A, WU C W. Hierarchically porous carbon derived from polymers and biomass: Effect of interconnected pores on energy applications [J]. *Energy & Environmental Science*, 2014, 7(11):3574-3592.
- [10] DENG J, LI M, WANG Y. Biomass-derived carbon: Synthesis and applications in energy storage and conversion [J]. *Green Chemistry*, 2016, 18(18): 4824-4854.
- [11] YAO Y, WU F. Naturally derived nanostructured materials from biomass for rechargeable lithium/sodium batteries [J]. *Nano Energy*, 2015, 17:91-103.
- [12] WU H, DENG Y, MOU J, et al. Activator-induced tuning of micromorphology and electrochemical properties in biomass carbonaceous materials derived from mushroom for lithium-sulfur batteries [J]. *Electrochimica Acta*, 2017, 242:146-158.
- [13] SHI G, YU M, LI R, et al. Graphene wrapped hair-derived carbon/sulfur composite for lithium-sulfur batteries [J]. *Journal of Materials Chemistry A*, 2015, 3(18):9609-9615.
- [14] ZHANG J, XIANG J, DONG Z, et al. Biomass derived activated carbon with 3D connected architecture for rechargeable lithium-sulfur batteries [J]. *Electrochimica Acta*, 2014, 116(2):146-151.
- [15] ZHANG Y. Optimization of extraction conditions of loquat leaf polysaccharide by water extraction and alcohol precipitation [J]. *Guizhou Agricultural Science*, 2014, 42:161-163. (in Chinese)
- [16] MI K, JIANG Y, FENG J, et al. Hierarchical carbon nanotubes with a thick microporous wall and inner channel as efficient scaffolds for lithium-sulfur batteries [J]. *Advanced Functional Materials*, 2016, 26(10):1571-1579.
- [17] ZHANG Z, LI Z, HAO F, et al. 3D interconnected porous carbon aerogels as sulfur immobilizers for sulfur impregnation for lithium-sulfur batteries with high rate capability and cycling stability [J]. *Advanced Functional Materials*, 2014, 24(17): 2500-2509.
- [18] LI J, QIN F, ZHANG L, et al. Mesoporous carbon from biomass: One-pot synthesis and application for Li-S batteries [J]. *Journal of Materials Chemistry A*, 2014, 2(34):13916-13922.
- [19] LI G, LI G, YE S, et al. A polyaniline-coated sulfur/carbon composite with an enhanced high-rate capability as a cathode material for lithium/sulfur batteries [J]. *Advanced Energy Materials*, 2012, 2(10):1238-1245.
- [20] LI Z, JIANG Y, YUAN L, et al. A highly ordered meso@microporous carbon-supported sulfur@smaller sulfur core-shell structured cathode for Li-S batteries [J]. *ACS Nano*, 2014, 8(9):9295-9303.
- [21] FERRARI A C, ROBERTSON J. Interpretation of Raman spectra of disordered and amorphous carbon [J]. *Physical Review B Condensed Matter*, 2000, 61(20):14095-14107.
- [22] FERRARI A C, BASKO D M. Raman spectroscopy as a versatile tool for studying the properties of graphene [J]. *Nature Nanotechnology*, 2013, 8(4): 235-246.
- [23] RENW, SAITO R, GAO L, et al. Edge phonon state of mono- and few-layer graphene nanoribbons observed by surface and interference co-enhanced Raman spectroscopy [J]. *Physical Review B*, 2010, 81(3):1718-1720.
- [24] MI K, CHEN S W, XI B J, et al. Sole chemical confinement of polysulfides on nonporous nitrogen/oxygen dual-doped carbon at the kilogram scale for lithium-sulfur batteries [J]. *Advanced Functional Materials*, 2017, 27(1):1604265.
- [25] XU R, LU J, AMINE K. Progress in mechanistic understanding and characterization techniques of Li-S batteries [J]. *Advanced Energy Materials*, 2015, 5(16):1500408.
- [26] YIN Yaxia, S Xin, GUO Yuguo, et al. Lithium-sulfur batteries: Electrochemistry, materials, and prospects [J]. *Angewandte Chemie International Edition*, 2013, 52(50):13186-13200.
- [27] LIN Z, LIANG C. Lithium-sulfur batteries: From liquid to solid cells [J]. *Journal of Materials Chemistry A*, 2014, 3(3):936-958.
- [28] ZHU L, ZHU W, CHENG X B, et al. Cathode materials based on carbon nanotubes for high-energy-density lithium-sulfur batteries [J]. *Carbon*, 2014, 75(8):161-168.
- [29] ZHAO M Q, ZHANG Q, HUANG J Q, et al. Unstacked double-layer templated graphene for high-rate lithium-sulphur batteries [J]. *Nature Communications*, 2014, 5(5):3410.
- [30] FANG R, ZHAO S, SUN Z, et al. More reliable

lithium-sulfur batteries: Status, solutions and prospects [J]. *Advanced Materials*, 2017, 29 (48): 1606823.

- [31] ZHANG J, HUANG M, XI B, et al. Systematic study of effect on enhancing specific capacity and electrochemical behaviors of lithium-sulfur batteries [J]. *Advanced Energy Materials*, 2018, 8 (2): 1701330.

Ms. **Luo Rui** received her B. S. degree in Chemistry from Chemical Institute of Chemical Industry in Liaocheng University in 2017. Now she is studying in Department of

Chemistry of Shandong University.

Prof. **Xiong Shenglin** received his Ph. D. degree in Chemistry from University of Science and Technology of China in 2007. From 2009 to 2011, he worked as a research fellow in Department of Chemical and Biomolecular Engineering of National University of Singapore. In 2017, he entered into School of Chemistry and Chemical Engineering at Shandong University as a professor. His research has focused on the basic research of inorganic synthesis and synthetic chemistry, especially in the synthetic methodology, precision synthesis and large-scale preparation of inorganic materials oriented by chemical energy storage.

(Executive Editor: Wang Jing)